I.FAST

Innovation Fostering in Accelerator Science and Technology

Horizon 2020 Research Infrastructures GA n° 101004730

DELIVERABLE REPORT

Fast-cycling Nuclotron HTS cable design

DELIVERABLE: D8.6

Document identifier:	IFAST-D8.6
Due date of deliverable:	End of Month 32 (December 2023)
Report release date:	16/02/2024
Work package:	WP8: Innovative superconducting magnets
Lead beneficiary:	GSI
Document status:	Final

ABSTRACT

The deliverable report reports on the developments for a high temperature superconductor cable for fast ramped applications. Based on an existing magnet design, mechanical properties of the superconductor and the achievable maximum cooling capacity, boundary conditions for the design of such a cable have been deduced.

For more information on IFAST, its partners and contributors please see https://ifast-project.eu/

This project has received funding from the European Union's Horizon 2020 Research and Innovation programme under Grant Agreement No 101004730. IFAST began in May 2021 and will run for 4 years.

Delivery Slip

	Name	Partner	Date
Authored by	T. Winkler, F. Gömöry, U. Zerweck-Trogisch	GSI, IEE, ILK	06.12.2023
Reviewed by	M. Vretenar [on behalf of Steering Committee]	CERN	16.02.2024
Approved by	Steering Committee		16.02.2024

TABLE OF CONTENTS

Executive summary

Based on an existing magnet design, requirements for cable parameters were determined. The work focused on three main topics: Cooling, Mechanics, and AC loss.

Thermal simulations were conducted based on the initial cable dimensions, establishing lower limits on the cooling channel diameter and upper limits on allowable AC loss. The mechanics of the tapes were investigated, setting further lower limits on the central cooling channel, and additional limits were established for the lay angle of the tapes.

Concerning AC loss, a simplified formula was developed. Based on the currently available HTS tape dimensions, this formula together with the results from the thermal simulations puts limits on the achievable ramp rates of a magnet. To reduce these losses, multiple strategies have been identified.

By making certain assumptions about the tape's cooling, simulations have been performed, indicating the feasibility of an HTS cable for fast-ramped applications.

1 Introduction

WP 8.6 aims to develop a high-temperature superconductor (HTS) nuclotron cable for fast-ramped high magnetic field applications. Over the last 32 months, the contributing parties have worked on this task, addressing the following main topics:

- Magnet Design
- Mechanics
- AC loss
- Cooling

Each partner has contributed to different topics based on their experience and skill sets. The goal was to establish parameters for designing and constructing an HTS nuclotron cable suitable for fast magnetic ramped applications, leveraging the direct cooling properties of its LTS variant. The forced flow of coolant in the hollow core of this cable type enables direct local cooling. Moreover, the round shape of the cable lacks a preferred bending direction, providing more flexibility in coil design.

However, the use of Niobium-Titanium in the nuclotron cable limits the performance of magnets built with this conductor. Therefore, this study aims to determine parameters for a cable using HTS. This is a challenging task due to the substantial differences in material properties between Niobium-Titanium and HTS.

In the initial step, the magnet design of an SIS300 dipole (using NbTi as a conductor) magnet is employed to establish goals for cable development.

2 Working Topics

2.1 Magnet Design

Starting point is the existing design of an SIS300 dipole magnet [1], [2]. Originally designed for a magnetic field of 4.5 T and cooled with supercritical helium, the requirement was increased to 6.5 T in the central bore for this development, based on user requests.

The list below outlines the basic parameters of a magnet using HTS:

- Accelerator Type: Fast-ramped single-aperture heavy-ion synchrotron
- Two-layer coil with 10 turns per pole
- Magnet length: 7.76 m
- Magnet curvature: 6 2/3°, with a radius of curvature: 66 m
- Operating temperature: 4 - 20 K
- Operating current: 30 kA
- Beam aperture: 85 mm

The magnet employs a cos-theta-coil design. For this coil type, the ends have a variable bending diameter depending on the respective position of the turns in the coil, see Figure 1. The innermost turn has the highest requirements for the bending radius of the cable. Based on the given requirements, it was calculated that the cable ideally should have a minimum bending radius of 20 mm.

Figure 1: Optimized design of the SIS300 dipole cos-theta-coil [3]. The different bending radii of the cable depending on the position of the cable in the winding pack is clearly visible.

Meeting this requirement poses a challenge. Therefore, a solution for the coil ends, similar to Figure 2, can be envisaged to circumvent this cable limitation. The figure illustrates the coil layout for one coil of a nested SIS100 steerer [4].

Figure 2: The coil layout depicts one coil of a nested SIS100 steerer coil. The primary coil layout follows that of a cos-theta magnet, but the coil heads are designed differently from the classical cos-theta design. This modification is necessary because two steerer magnets are nested into each other for this magnet, combining both horizontal and vertical steering capabilities.

Figure 3 illustrates a magnetic field calculation for the magnet. Although this coil layout has not been optimized for magnetic field harmonics, it served as a starting point for determining the cable requirements.

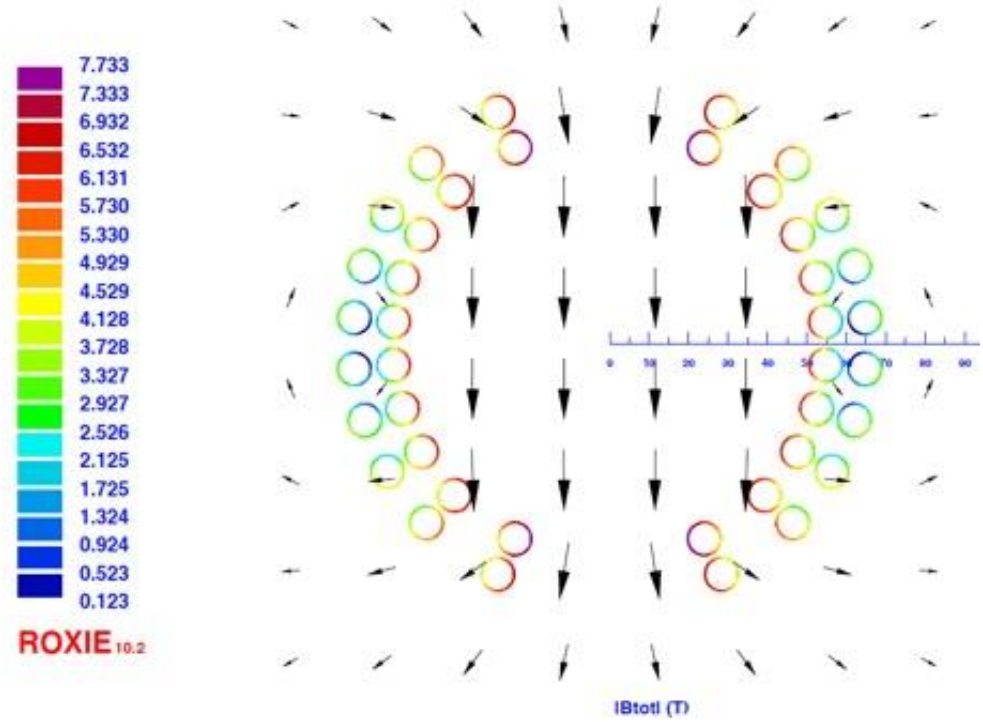

Figure 3: Simulation of the magnetic field for the cross-section of a cos-theta magnet, assuming a 30 kA current in the cable. Please note: This design is not optimized and should only be used as an indication..

Based on the existing magnet design, it can be inferred that the cable length requirement for one pole is 200 m. This serves as one boundary condition for the cable cooling.

2.2 COOLING ASPECTS

The goal is to leverage the effective local cooling achievable through forced flow cooling. In this scenario, the cooling channel diameter becomes a crucial variable, as it influences the pressure drop and, consequently, the mass flow of coolant.

Investigations were conducted for a range of inlet and outlet conditions, calculating the achievable cable length. One finding from these investigations is that cooling with liquid or sub-cooled liquid, as used for SIS100 magnets, is insufficient to cool 200 m long cables.

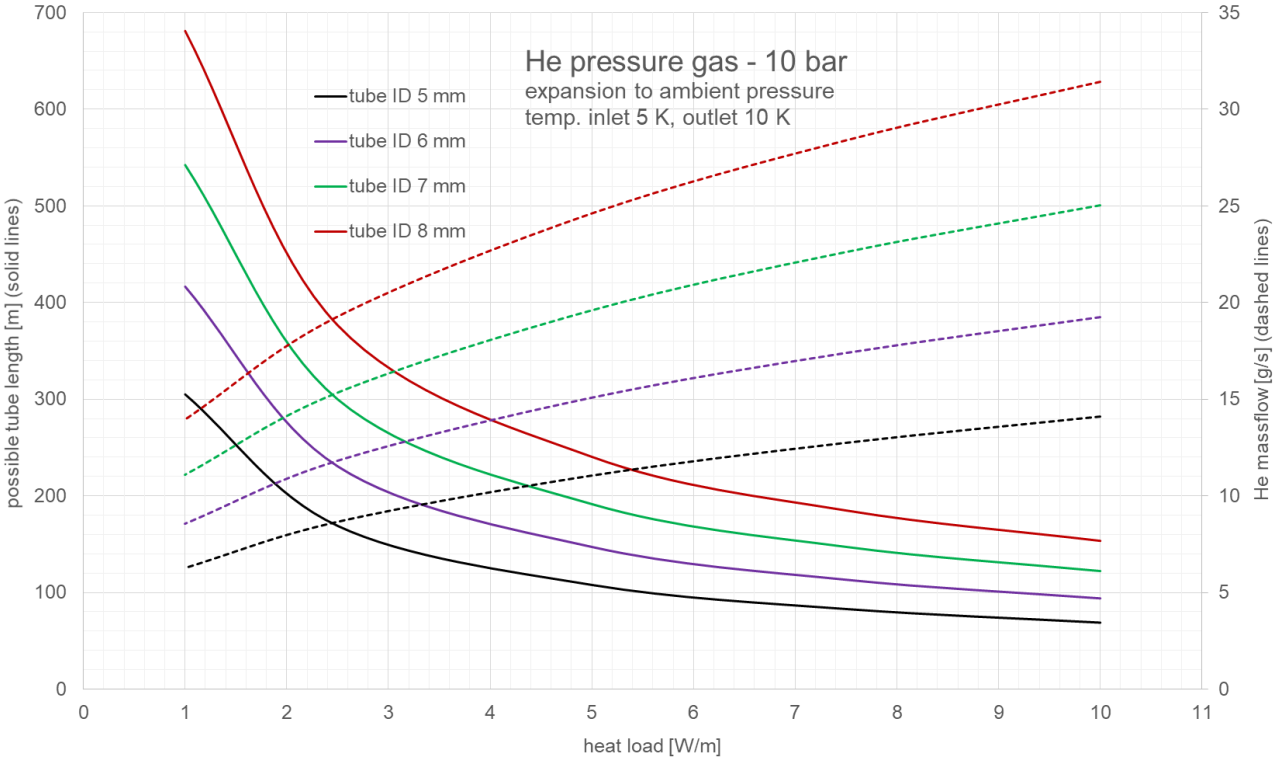

Figure 4: Possible cooling channel lengths for different AC losses are depicted. Supercritical helium at an inlet pressure of 10 bar (abs) and a temperature of 5 K is assumed, with the outlet temperature set at 10 K. The diagram enables the reading of potential cooling channel lengths and resulting mass flow for given channel diameters and introduced AC losses..

As an alternative, the use of supercritical helium was numerically investigated. Using helium at 10 bar and 5 K as inlet conditions, a 200 m long cable can be cooled, assuming AC losses lower than 6.5 W/m (see Figure 4) , with a maximum temperature at the outlet of the cooling channel assumed to be 10 K. Higher allowable outlet temperatures increase the heat load that can be handled at a given length.

2.3 MECHANICAL ASPECTS

As a result of their manufacturing process, HTS tapes have a multi-layered architecture. Simultaneously, the superconducting properties of the tapes strongly depend on the applied

stress/strain. Since multiple tapes are wrapped around a central cooling channel during the cable manufacturing process, it is crucial to determine the minimum bending diameter of a tape around the cooling channel. This bending diameter establishes lower limits on the diameter of the cooling channel, consequently restricting the minimum bending diameter for the cable in the coil ends.

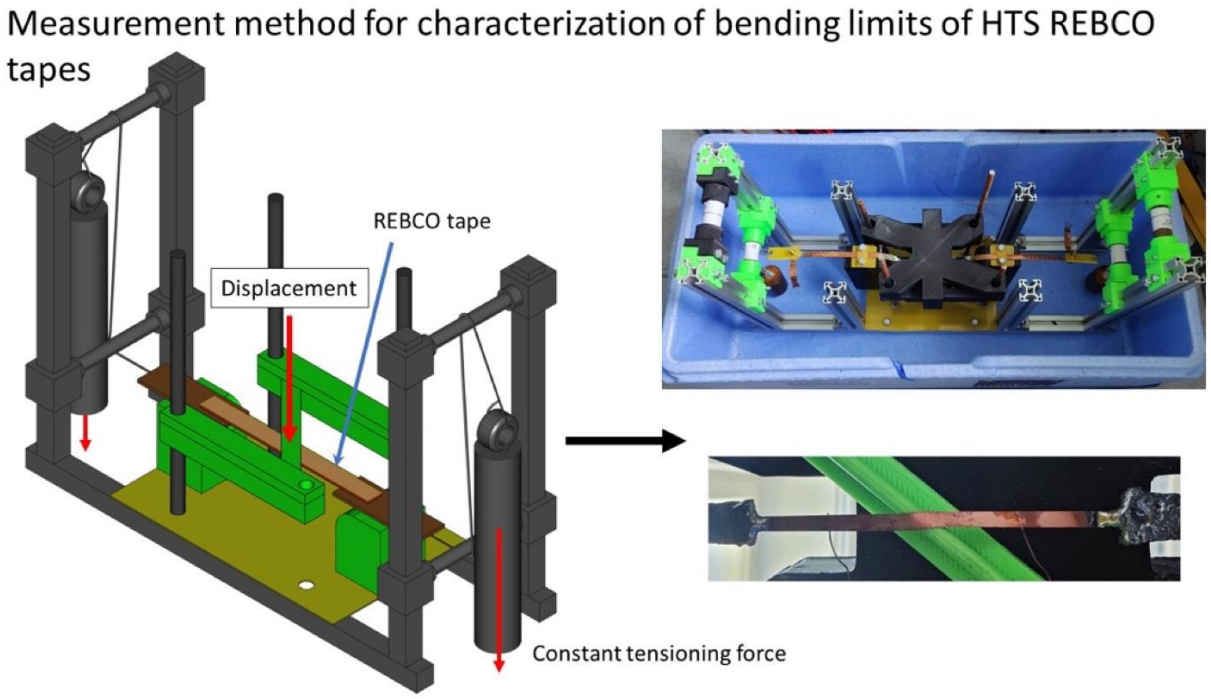

Figure 5: Schematic view of the setup for the characterization of bending limits of HTS tapes. It keeps the tapes under a determined tension while allowing to vary the angle of the displacement piece.

IEE conducted a series of tests with tapes from different manufacturers using a dedicated setup to assess the transporting capability of deformed tapes immersed in liquid nitrogen, see Figure 5. A pressing tool with a round imprinting surface was applied against the wide face of the tape at a constant force, and the critical current was measured upon reaching the state of the investigated deformation.

Tests were performed for three angles between the tape and the imprinting tool: 30°, 45°, and 60°, as can be seen in Figure 6.

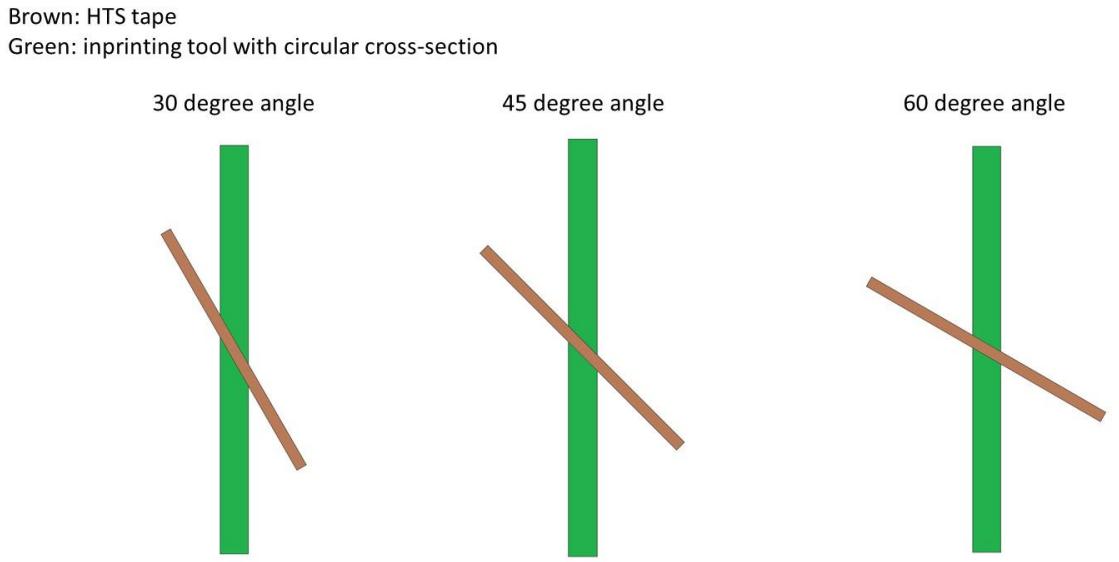

Figure 6: Schematic view of the three different angles between former and tape that were investigated.

Tapes from two different manufacturers were tested, and the main characteristics are provided in Table 1 below:

Table 1: List of tape parameters from Theva [5] and Shanghai Superconductor Technology Co. Ltd. [6] used in the experiments.

THEVA 4301 Pro Line	
Width	3 mm
Buffer Layer	3.5 µm
REBCO layer	3.1 µm
Substrate layer	100 µm
Silver layers (top and bottom	2 µm
Copper layers (top and bottom)	10 µm

Shanghai Superconductor Technology	
Width	3 mm
Buffer Layer	some nm
REBCO layer	2 µm
Substrate layer	30 µm
Silver layers (top and bottom	2 µm
Copper layers (top and bottom)	5 µm

The results of these tests for the Shanghai tape are presented in Figure 7. As expected, the bending resulting in compression of the HTS layer (tape oriented inwards the cable) is less demanding than the tension at the HTS layer facing outward.

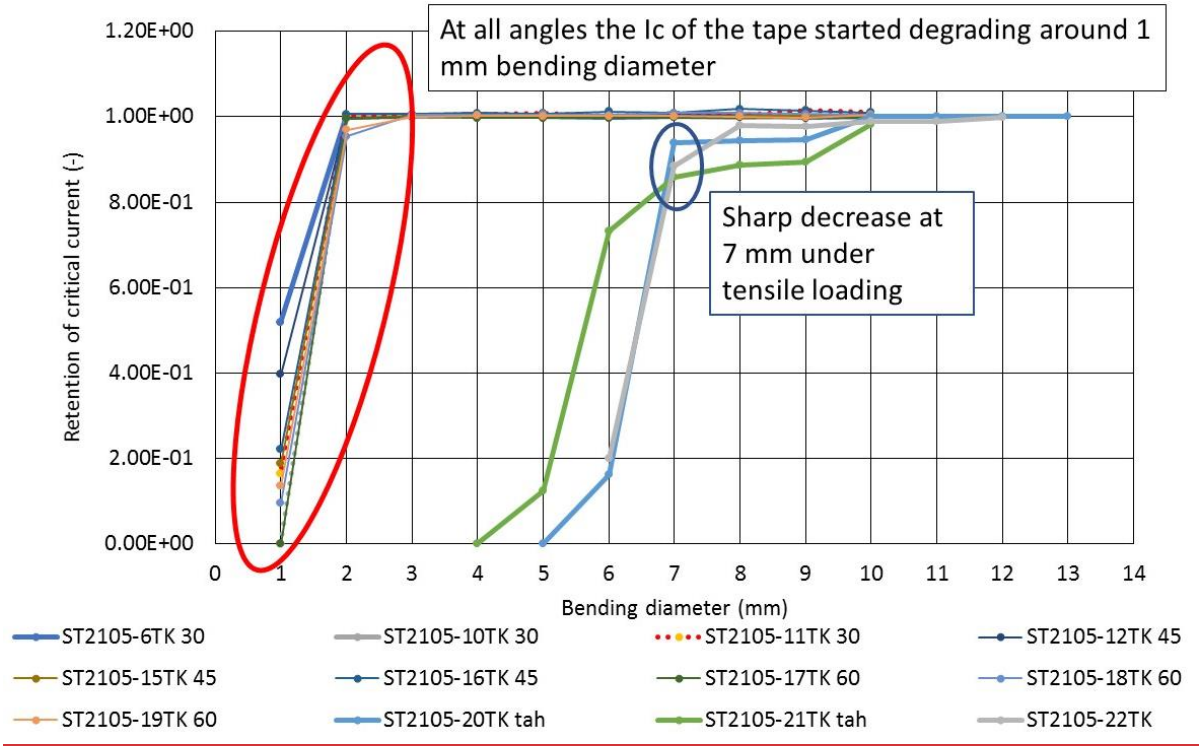

Figure 7: Measurement results for the bending experiments conducted by Shanghai Superconductor Technology Co. Ltd. Two distinct groups of curves are readily identifiable: one for experiments where the HTS layer is under compression and another for tensile loading of the HTS tape.

The tape manufactured by THEVA indicates slightly lower resilience towards bending, as can be seen in Figure 8.

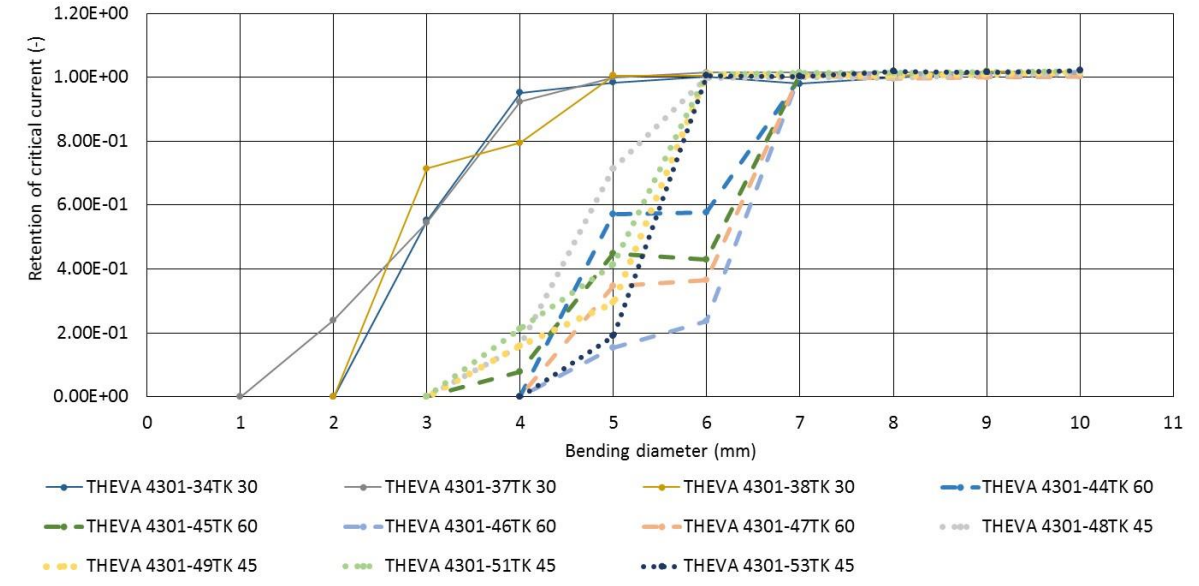

Figure 8: Bending test results for HTS tapes from Theva. Two main families of curves can be seen, one for compressive loading and one for tensile loading. In subgroups also a dependency on the lay angle can be identified.

Based on these tests, the lower limit of 7 mm for the central cooling channel has been established.

2.4 AC Loss

One main input parameter for the thermo-hydraulic calculations is the expected heat load in the cable. For HTS tapes, and as a consequence, cables made with HTS tapes, this loss is predominantly due to the hysteresis curve. The following formula was developed and used to get an estimate of the hysteresis loss of a cable made from helically wound HTS tapes:

$$Q_{hT} = \frac{2}{\pi cos\alpha} B_{max} I_c w$$

This loss formula has one free parameter—the HTS tape width—with the two variables $N * I_c$ and B_{max} resulting from the global requirements of the magnet. The validity of this formula for magnetic fields above full penetration was experimentally verified at 4 K and 77 K.

For a cable made from 4 mm wide tapes, a common commercially available tape width, and a 45° lay angle, this leads to an AC loss of 373 J/cycle m when ramping from injection (1.9 T) to extraction (7.5 T). In initial thermal simulations for magnet cooling circuits, this was found to result in cable temperatures above the critical temperature of HTS.

As countermeasures, the following topics were identified:

- Higher operating temperatures
- Allow temperature swings during operation
- Reduction of HTS width
- Reduced ramp rates
- Adapted cable designs, moving away from round wires (outside the scope of this R&D activity)

For the above-mentioned solutions, thermal simulations were set up with the following parameters:

- Extend ramp duration from 1 sec to 10 sec
- Allow a higher operating temperature during ramping
- Tapes with 4 mm width and 0.5 mm wide HTS filaments

The first measure will extend the time over which heat is generated in the tape, reducing the W/m. The second measure means that at the start of the ramp, the cable is cold; during ramping, the cable and the coolant will warm up, and after the ramp, during the plateau, the cable will be cooled down again. This allows for the materials to work as a thermal buffer. The third measure will reduce the hysteresis loss by a factor of 8.

With the measures above the AC loss power density is reduced from 373 W/m to 4.6 W/m, a reduction by about 88%.

For assessing the temperature distribution in a cooling channel and the individual HTS layers during ramping, the thermal resistances have to be known. They serve as a basis to calculate the

temperature gradient between the cooling channel and the outermost HTS layer of the CORC.

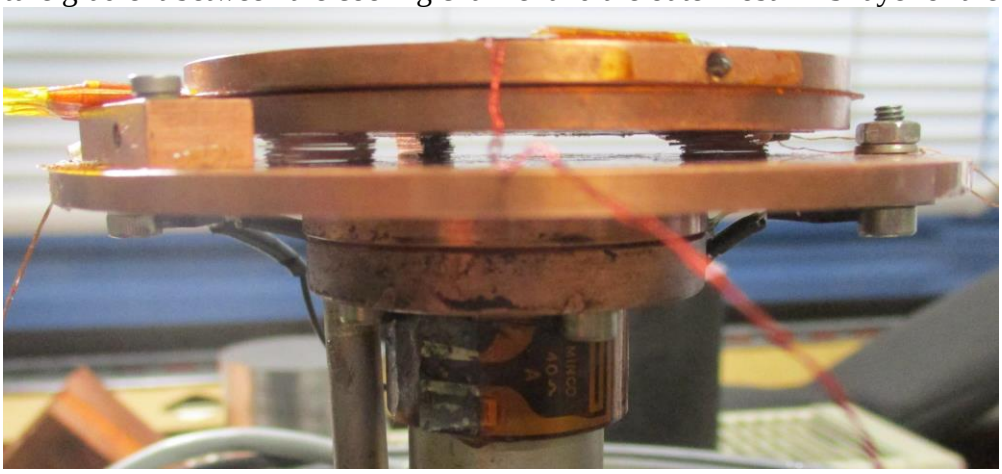

Figure 9: Side view of three stacks, each consisting of 25 HTS strips, used for heat conductivity measurements. The mechanical treatment of the HTS results in warped edges, causing visible gaps when stacked. Applying an additional weight of 2 kg compressed the three stacks during the heat conductivity measurement, effectively reducing the gaps between layers.

To evaluate the heat conductivity of HTS stacks in a CORC three stacks of 25 HTS strips each were measured (see Figure 9). The heat conductivity between individual strips yielded to be $\lambda = 0.17 \frac{W}{m\,K}$ at 50 K. At lower temperatures of around 10 K, $\lambda = 0.15 \frac{W}{m\,K}$ would be a reliable value. Deformed edges of the HTS strips led to visible gaps between the sheets, this reduces the heat conductivity dramatically in (insulation-)vacuum. On the other hand, when winding a CORC there will also be vacuum-filled gaps between the individual HTS layers, see *Figure 11*.

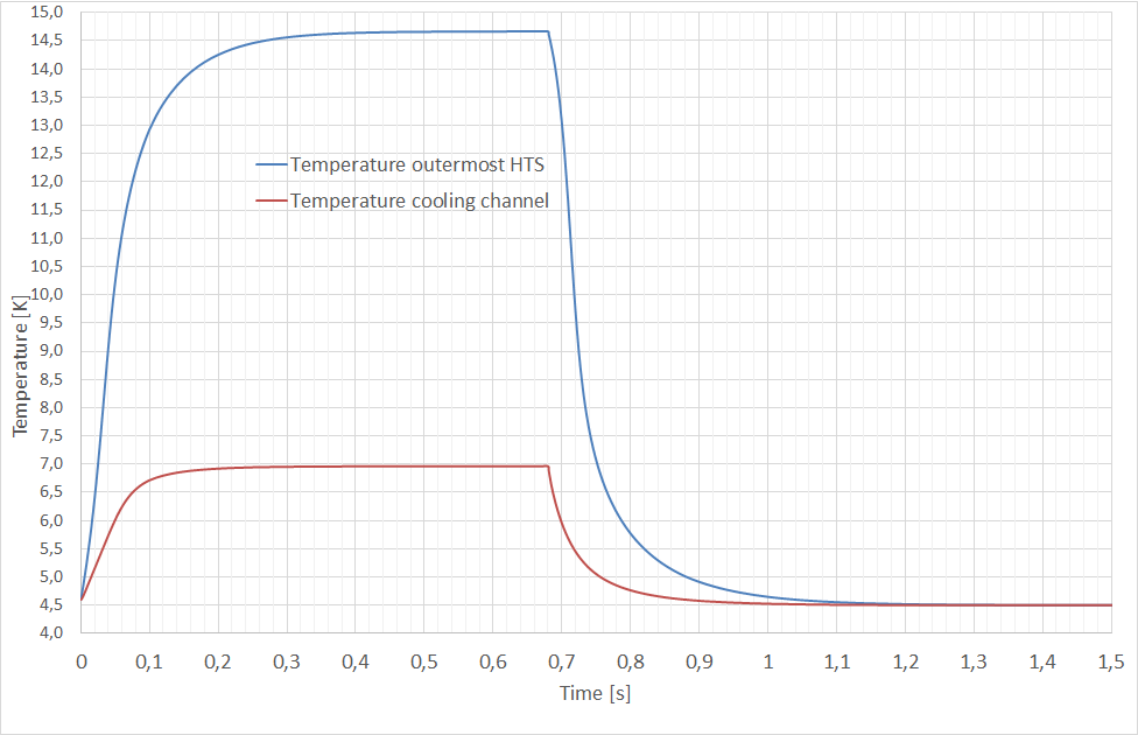

Figure 10: Time-dependent temperature of the cooling channel and the outermost HTS layer at an AC loss heat load of 27 W/m during and after current ramping for 0.7 s.

Due to the low thermal conductivity between individual HTS sheets, the time-dependent temperature evolution was calculated when the magnet current is ramped at the nominal speed, introducing AC losses heat. As the temperatures settle quite quickly, the ramping time in the simulation was reduced, introducing a heat load of 27 W/m for only 0.7 seconds for a comprehensive diagram. As seen in Figure 10, the temperatures rise during the current ramp, reaching below 15 K for the outermost HTS layer. On the other hand, all temperatures settle within 0.4 seconds close to 4.5 K after terminating the current ramp.

The radial temperature distribution over the individual HTS layers wrapped around the cooling channel is color-coded in *Figure 11*, with the cooling channel temperature (7 K) below the color scaling. While the 1st layer shows no gaps between individual HTS bands, subsequent layers generate vacuum-filled gaps due to the increasing former diameter. These gaps reduce the effective heat transition for higher layer numbers, leading to increased heat resistance and thus increased temperatures during ramping.

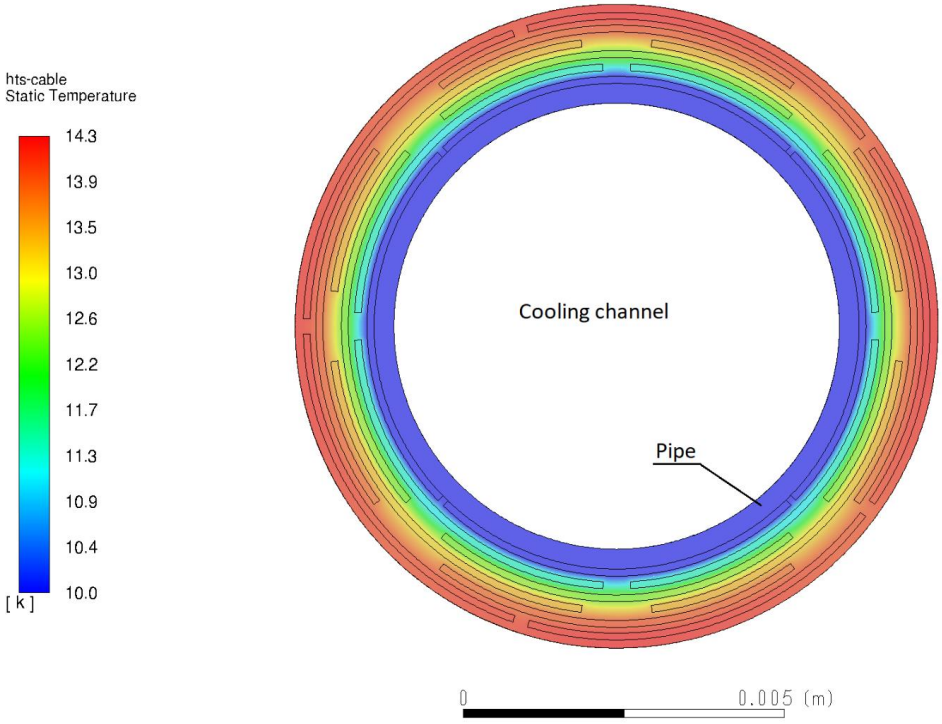

Figure 11: Radial temperature distribution of the different HTS layers, wrapped around the cooling channel. Please also note that there will be insulation-vacuum filled voids between the individual HTS layers which hamper the otherwise good thermal conductivity of the HTS itself.

3 Conclusion

In the context of this work package, a foundational set of parameters for an HTS nuclotron cable has been identified. The predominant challenge facing the cable's viability lies in the elevated AC losses associated with commercially available tapes. Addressing this issue involves exploring innovative solutions, such as incorporating striation to effectively reduce the width of the superconductor. Additionally, there is a need to embrace significantly higher temperature swings between the ramp and plateau operation phases. The culmination of these efforts has yielded a set of parameters that

pave the way for the manufacturing of an extended prototype cable. Looking ahead, the next crucial step involves the winding of a longer cable, subsequently coiling it into a solenoid configuration for more in-depth investigation and evaluation.

4 References

[1] P. Fabbricatore *et al.*, "The Curved Fast Ramped Superconducting Dipoles for FAIR SIS300 Synchrotron: From First Model to Future Developments," *IEEE Trans. Appl. Supercond.*, vol. 23, no. 3, pp. 4000505–4000505, Jun. 2013, doi: 10.1109/TASC.2012.2229332.

[2] P. Fabbricatore *et al.*, "Development of a Curved Fast Ramped Dipole for FAIR SIS300," *IEEE Trans. Appl. Supercond.*, vol. 18, no. 2, pp. 232–235, Jun. 2008, doi: 10.1109/TASC.2008.922291.

[3] B. Auchmann, S. Russenschuck, and N. Schwerg, "Discrete Differential Geometry Applied to the Coil-End Design of Superconducting Magnets," *IEEE Trans. Appl. Supercond.*, vol. 17, no. 2, pp. 1165–1168, Jun. 2007, doi: 10.1109/TASC.2007.897233.

[4] K. Sugita, E. Fischer, H. Khodzhibagiyan, and J. Macavei, "Design Study of Superconducting Corrector Magnets for SIS 100," *IEEE Trans. Appl. Supercond.*, vol. 20, no. 3, pp. 164–167, Jun. 2010, doi: 10.1109/TASC.2009.2038716.

[5] "Welcome to THEVA GmbH - your manufacturer of 2G HTS wire," THEVA english. Accessed: Dec. 05, 2023. [Online]. Available: https://www.theva.com/

[6] "Shanghai Superconductor Technology Co., Ltd." Accessed: Dec. 05, 2023. [Online]. Available: http://www.shsctec.com/index.php?m=list&a=index&classid=51